UDK 669.715:66.065.32
Original scientific article/Izvirni znanstveni članek

ISSN 1580-2949
MTAEC9, 56(2)225(2022)

THERMAL-DEFORMATION MODEL OF A Sr-MODIFIED A356 ALUMINUM ALLOY

MODEL TERMIČNE DEFORMACIJE S STRONCIJEM MODIFICIRANE ALUMINIJEVE ZLITINE VRSTE A356

Yongyue Liu[1,2,3], Xianglai Xu[1], Jiangxiong Cheng[1], Hongwei Sun[1], Xueping Ren[1*], Peng Jiang[2]

[1]School of Materials Science and Engineering, University of Science and Technology Beijing, Beijing, 100083 China
[2]Forging Technology Center, Beijing Research Institute of Mechanical and Electrical Technology Beijing, 100083, China
[3]Technology Center, Ningbo Heli Technology Shareholding Co. Ltd, Ningbo, 315700, China

Prejem rokopisa – received: 2021-01-06; sprejem za objavo – accepted for publication: 2022-03-03

doi:10.17222/mit.2022.355

The hot-deformation behavior of A356 aluminum alloy with a Sr modification was investigated using a Gleeble 1500 thermal simulator. The true stress-strain curves with a deformation temperature of 300–500 °C and a strain rate of 0.01–5 s^{-1} were clarified. The activation energy of the A356 aluminum alloy with Sr modification was 221.474 kJ/mol. The influences of friction and temperature on the curves were investigated, and then the constitutive equation was established. The results show that the flow stress is obviously affected by temperature and strain rate. The experimental stress is lower than the theoretical stress, and the stress difference between the experimental and theoretical stress increases with the increasing strain. The maximum stress difference reaches 17.8 MPa when the sample deformed at 300 °C/5 s^{-1} with a reduction of 16 %. For all the deformation conditions the correlation coefficient is 0.99 and the average relative error is 4.8 %, which shows the good predictability of the current model. The developed constitutive equation can provide guidance for the study of the hot-deformation behavior of similar aluminum alloys.

Key words: A356 aluminum alloy, Sr modification, microstructure, thermal-deformation model

Avtorji v članku opisujejo raziskavo obnašanja Al zlitine vrste A356, modificirane s stroncijem (Sr) med vročo deformacijo na termo-mehanskem simulatorju Gleeble–1500. Določili so krivulje *napetost-deformacija* pri temperaturah deformacije med 300 °C in 500 °C in hitrostih deformacije med 0,01 s^{-1} in 5 s^{-1}. Aktivacijska energija izbrane Al zlitine A356 modificirane s Sr je približno 221,5 kJ/mol. Ugotavljali so vpliv trenja in temperature na krivulje in nato določili konstitutivne enačbe. Rezultati raziskave so pokazali, da na napetost tečenja vpliva temperatura in hitrost deformacije. Eksperimentalno ugotovljena napetost je nižja kot teoretično določena in razlika med njima narašča z naraščanjem deformacije. Maksimalna napetostna razlika ima vrednost 17,8 MPa, ko je bil preizkušanec deformiran pri 300 °C s hitrostjo deformacije 5 s^{-1} in 16 % redukcijo preseka preizkušanca. Pri vseh pogojih deformacije je bil koeficient korelacije 0,99 in povprečna relativna napaka 4,8 %, kar kaže na dobro ujemanje izdelanega modela z eksperimenti. Razvita konstitutivna enačba je lahko napotek drugim pri študiju vroče deformacije podobnih Al zlitin.

Ključne besede: zlitina na osnovi Al vrste A356, modifikacija s stroncijem, mikrostruktura, model termične deformacije

1 INTRODUCTION

Due to its desirable performance in casting, fatigue, and corrosion, as well as the excellent combination of strength and toughness, the A356 aluminum alloy is widely used in the aerospace and automotive industries.[1–6] Owing to the proper components of Al and Si elements, as well as the reasonable heat-treating process, the A356 aluminum alloy usually contains an Al-enriched phase and eutectic Si particles.[7] However, the Si particles probably grow into a needle-liked shape, leading to a dramatic decrease of the ductility.[8,9]

To reduce the deleterious effect brought about by the needle-liked Si particles, modification elements, e.g., rare-earth elements[10] and Sr, were added to the A356 aluminum alloy. Tsai et al. found that the rare-earth element La could improve the mechanical properties of the A356 aluminum alloy.[11] However, the rare-earth elements could promote the formation of coarsened α-Al grains and the Al-Si-La compounds, bringing about an inhomogeneous microstructure. In contrast, the Sr element can modify the needle-liked Si particles into a fibrous structure with finer grains.[12] This effect is called eutectic modification and it could improve the performance of the A356 aluminum alloy. Researchers have investigated the influence of Sr on the tensile strength, fatigue life, and shock strength of the A356 aluminum alloy.[1,12] However, the thermal deformation behavior of the A356 aluminum alloy modified by Sr has not been studied systematically.

Therefore, the current study aims to clarify the thermal deformation behavior of the A356 aluminum alloy modified by Sr. Schematic thermal compression tests were carried out to investigate the hot-deformation characteristics. A mechanisms-based material constitutive model was established by modifying the effects of friction and the deformed temperature. The developed material model can be further implemented into the research

*Corresponding author's e-mail:
rxp33@ustb.edu.cn

Table 1: Chemical composition of the experimental A356 aluminum alloy (*w*/%)

Si	Fe	Cu	Mn	Mg	Cr	Ni	Zn	Ti	Sr	Al
6.87	0.091	< 0.001	0.034	0.363	0.006	0.004	0.004	0.207	0.0235	Bal.

on the thermal deformation of the aluminum alloys and provide guides for manufacturing aluminum alloy parts, which are widely applied in aerospace and automotive industries.

2 EXPERIMENTAL PART

The material used was an A356 aluminum alloy modified by Sr. An ingot of the experimental aluminum alloy with the measured chemical composition (**Table 1**) was prepared in a vacuum gravity casting furnace. Samples with the size of ϕ 8 mm × 15 mm were machined from the center of the ingot.

The isothermal hot-compression tests were carried out on a Gleeble 1500 thermal simulator. The final deformation degree was set to 50 %. The specimens were heated to the target temperature with a heating rate of 5 °C/s. After being homogenized for 2 min, the specimens started to access the thermal deformation stage. The deformation temperatures were (300, 350, 400, 450, 500 and 550) °C, and the initial strain rates were (0.01, 0.1, 1.0 and 5.0) s^{-1}. Then the deformed samples were quenched rapidly to room temperature with cold water. The temperature was monitored in real time and controlled by a thermocouple that welded on the samples, while liquid lubricant and graphite flake were applied to reduce the friction between the sample and the fixture.

3 RESULTS AND DISCUSSION

3.1 Microstructures of the A356 aluminum alloy after thermal compression tests

The microstructure of the experimental material consists of α-Al and eutectic Si, as shown in **Figure 1.**

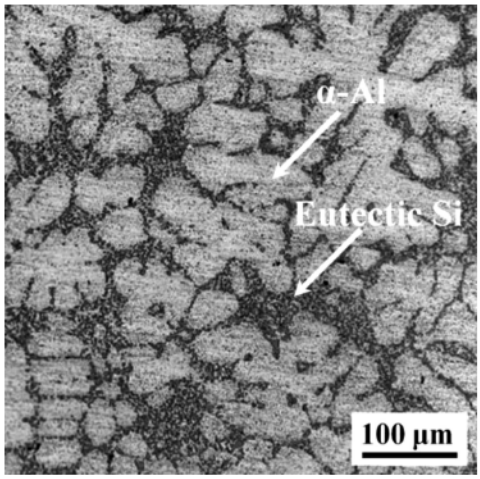

Figure 1: Microstructure of the experimental A356 aluminum alloy

After the test, the tissue structure of the material changed. **Figure 2** shows the microstructures of the A356 after thermal compression tests at 300–500 °C with an initial strain rate of 5.0 s^{-1} and 0.01 s^{-1}. It was found that the original grains of the α-Al were squashed along the compression direction and the fine grains of eutectic Si showed a streamlined distribution along the grain boundaries of the α-Al. The eutectic Si particles are precipitated by equiaxed (or quasi-equiaxed) morphology, which has more positive effect on the ductility of the alloy compared to the needle-liked morphology. The strain rate has little effect on both the size and the morphology of the Al grains. The grain size of α-Al decreased when the deformation temperature increased from 300 °C to 350 °C, then it enlarged when the deformation temperature further increased to 500 °C.

3.2 The influence and modification of friction

The experimental true stress-strain curves are shown as the solid lines in **Figure 3**. The true stress increased dramatically at the original stage and subsequently re-

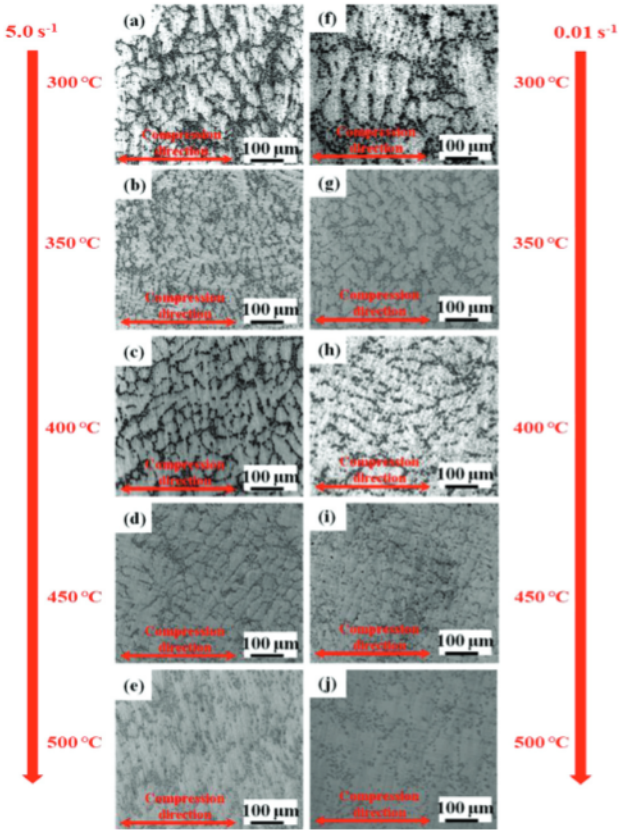

Figure 2: Microstructures of the A356 aluminum alloy after thermal compression tests using different process parameters

mained stable with the increase of the true strain. The flow stress decreased with the elevation of the deformation temperature, while it increased with the increase of the strain rate.

The lubricant cannot eliminate the friction between the sample and fixture, which affects the deformation of the contacted surfaces on the sample, contributing to the inhomogeneous deformation of the samples. As the friction can change the theoretical curve, the effect of friction on the theoretical curve of the A356 aluminum alloy was modified according to Equations (1) to (4):[13,14]

$$\sigma = \frac{\sigma_0 C^2}{2(\exp C - C - 1)} \tag{1}$$

$$C = \frac{2\mu R}{h} \tag{2}$$

$$\mu = \frac{\frac{R_1}{h_1} b}{\frac{4}{\sqrt{3}} - \frac{2b}{3\sqrt{3}}} \tag{3}$$

$$b = 4\frac{\Delta R}{R_1} \cdot \frac{h_1}{\Delta h} \tag{4}$$

where σ_0 and σ are the experimental flow stress before and after the modification of friction, respectively; R_0, R and R_1 are the initial, instant, and final radius of the samples, respectively, and $R = R_0\sqrt{h_0 / h}$, $R_1 = R_0\sqrt{h_0 / h_1}$; h_0, h and h_1 are the initial, instant, and final height of the samples, respectively; ΔR is the difference between the maximum radius (R_M) and the radius of the surfaces (R_T) after deformation; Δh represents the variation of height before and after the deformation; μ represents the friction factor.

The friction factor μ was calculated from the measured R_M, R_T and h_1. The instant height h was measured using the L-Gauge module of the Gleeble–1500 thermal simulator, and the instant radius R was calculated according to h. All the parameters above were taken into the Equation (1), and the true stress – strain curves modified are shown as the dotted lines in **Figure 3**.

Figure 3 shows that the friction-corrected curve is lower than the original true stress-strain curve, and the variation increased with the increase of the deformation degree. This phenomenon is because of the inhomogeneous distribution of the lubricant during the deformation process, which brings the increase in the friction and changes the flow stress. It can also be observed that friction has different effects on stress under different deformation temperatures and strain rates. Generally, the lower the temperature and the higher the strain rate, the greater effect of the friction obtained. The improvement

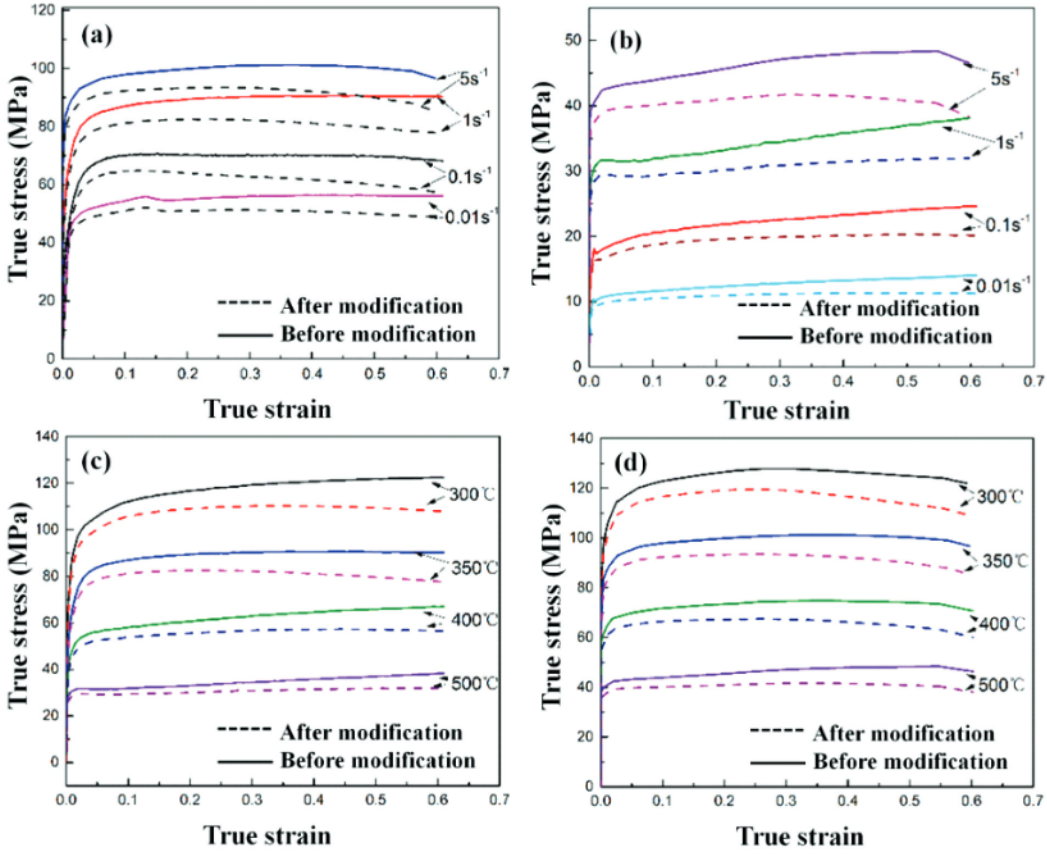

Figure 3: True stress-strain curves of the A356 aluminum alloy during the thermal compression process before and after the friction correction: a) at 350 °C, b) at 500 °C, c) at 1 s^{-1}, d) at 5 s^{-1}

of temperature could reduce the strength and the effect of friction.

3.3 The adiabatic temperature correction

The friction-modified stress-strain curves of the samples deformed at 300 °C are shown in **Figure 4a.** Most of the energy in the metals will transfer to thermal energy during the plastic deformation process.[15] When the deformation rate is lower, e.g., less than 1 s^{-1}, the generated heat could be released to the environment instantly, thus the measured temperature illustrates waves; when the deformation rate is higher, e.g., 5 s^{-1}, the generated heat gathered in the sample, resulting in the increase of temperature, as shown in **Figure 4b**. Therefore, the effect of actual temperature on the true stress-strain curve should be modified.

The increase of temperature at a high strain rate could be calculated by Equation (5)[16]:

$$\Delta T = \frac{\eta W \int_{\sigma} \mathrm{d}\varepsilon}{\rho C} \tag{5}$$

where ΔT and $\int_{\sigma} \mathrm{d}\varepsilon$ are the increase of temperature and mechanical energy during the deformation, respectively; ρ, C, W are the ratio that density, specific heat capacity, and mechanical energy transferred into the heat energy, which are 0.9–0.95; η is adiabatic factor, defined as the ratio between the actual increase of temperature and the increase of temperature under adiabatic condition.

The effect of the temperature wave on the flow stress ($\Delta\sigma$) could be calculated by Equation (6):[17]

$$\Delta\sigma = \frac{Q}{n\alpha R}\left(\frac{1}{T} - \frac{-1}{T+\Delta T}\right) \tag{6}$$

where Q and R are the activation energy of the deformation and gas constant, respectively; n and α are the material parameters. The hyperbolic sine model was applied to solve the Q, n and α:[9]

$$\dot{\varepsilon} = AF(\sigma)\exp\left(-\frac{Q}{RT}\right) \tag{7}$$

where $F(\sigma)$ is a function of the stress, and it can be generally calculated by (7) under low stress, calculated by Equation (8) under high stress, and calculated by Equation (9) in general:

$$F(\sigma) = \sigma^{n_1}, \quad (\alpha\sigma) < 0.8 \tag{8}$$

$$F(\sigma) = \exp(\beta\sigma), \quad (\alpha\sigma) > 1.2 \tag{9}$$

$$F(\sigma) = [\sinh(\alpha\sigma)]^{n} \tag{10}$$

where A, α, β, n and n_1 are parameters of the material, and $\alpha = \beta/n_1$.

Combining Equations (10), (11) and (12) to Equation (8), the relationship between and σ can be obtained:

$$\dot{\varepsilon} = A_1\sigma^{n_1}\exp\left(-\frac{Q}{RT}\right) \quad (\alpha\sigma) < 0.8 \tag{11}$$

$$\dot{\varepsilon} = A_2\exp(\beta\sigma)\exp\left(-\frac{Q}{RT}\right) \quad (\alpha\sigma) > 1.2 \tag{12}$$

$$\dot{\varepsilon} = A[\sinh(\alpha\sigma)]^{n}\exp\left(-\frac{Q}{RT}\right) \tag{13}$$

Taking a logarithm on both sides of Equations (11), (12) and (13):

$$\ln\dot{\varepsilon} = \ln A_1 - \frac{Q}{RT} + n_1 \ln\sigma \tag{14}$$

$$\ln\dot{\varepsilon} = \ln A_2 - \frac{Q}{RT} + \beta\sigma \tag{15}$$

$$\ln\dot{\varepsilon} = n\ln[\sinh(\alpha\sigma)] + \ln A - \frac{Q}{RT} \tag{16}$$

The Equations (14) and (15) illustrate the linear relationship of ln-lnσ and ln-σ, respectively. Since the flow stress curve confirms the dynamic recovery, the maximum of the flow stress reached when the strain is low, and then kept stable. The fitting curves of the related pa-

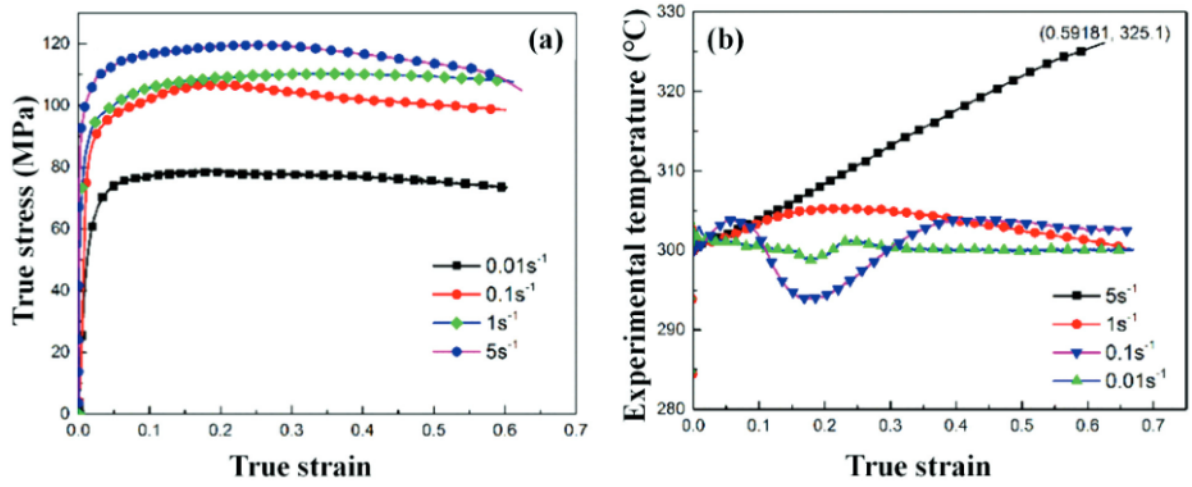

Figure 4: Effect of adiabatic temperature rise on the flow stress of the A356 aluminum alloy: a) true stress-strain curves at 300 °C, b) measured temperature curves

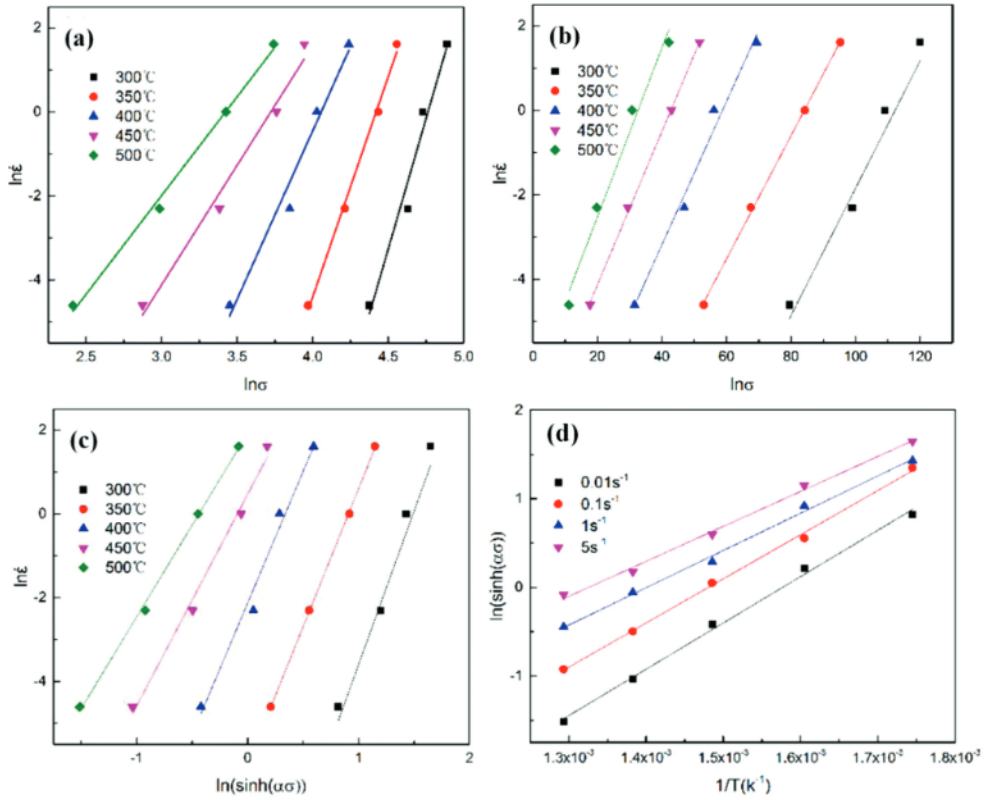

Figure 5: Fitting curve of each parameter: a) n_1, b) β, c) n, d) Q

rameters are displayed in **Figure 5**. The values $n_1 = 8.6567$, $\beta = 0.1695$, $\alpha = 0.01958$, $n = 5.9226$ and $Q = 226.1138$ kJ/mol can be obtained.

Based on the above results, the effect of temperature on the true stress-strain curves were modified. The curves when the strain rate is 5 s^{-1} are shown in **Figure 6**. It can be observed that the strength of the alloy decreased with an increase of temperature. That is to say, a higher temperature could promote the softening of the flow stress. The experimental stress is lower than the theoretical value, and the distinction increased with the increase of the strain. The largest variation reaches 17.8 MPa when the sample deformed at 300 °C and 5 s^{-1}, with a decrease of 16 %.

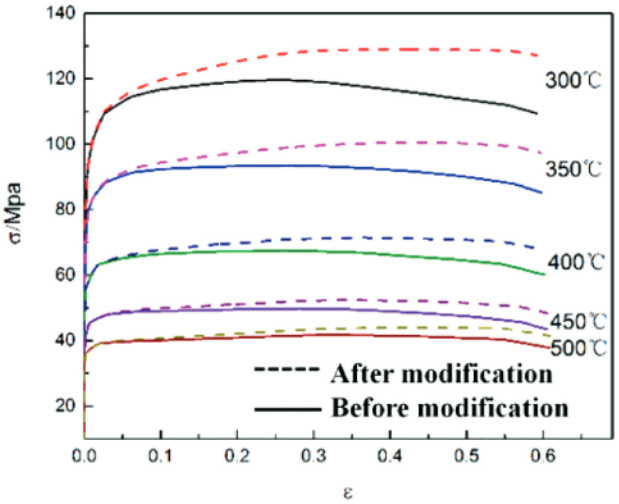

Figure 6: True stress-strain curves of the A356 aluminum alloy during thermal compression process before and after the modification of temperature at a strain rate of 5 s^{-1}

When the deformation temperature is lower, e.g., at 300 °C, the stress decreases after getting to the peak of the stress, where it undergoes conventional deformation. With the improvement of temperature, the stress level decreases dramatically and then keeps stable, e.g., at 500 °C. This phenomenon is because of the temperature arrives the critical value of generating superplastic deformation.[18] What is more, the deformation mechanism arises from the combination effect of conventional and superplastic deformation.

3.3 The constitutive equation with a consideration of strain

It can be seen from Equation (16) that ln$A$ is the intercept of the lnZ-ln[sinh($\alpha\sigma$)] relationship. Based on the stress-strain relationships after modification of the friction and temperature as shown in **Figure 7** ($\varepsilon = 0.1$), the values $n = 5.7934$, $Q = 221.474$ kJ/mol, $\alpha = 0.01937$, and $A = 1.894 \times 10^{16}$ can be obtained. This model contains the parameter Z, which evaluates the effects of temperature and strain rate on the mechanical behavior:

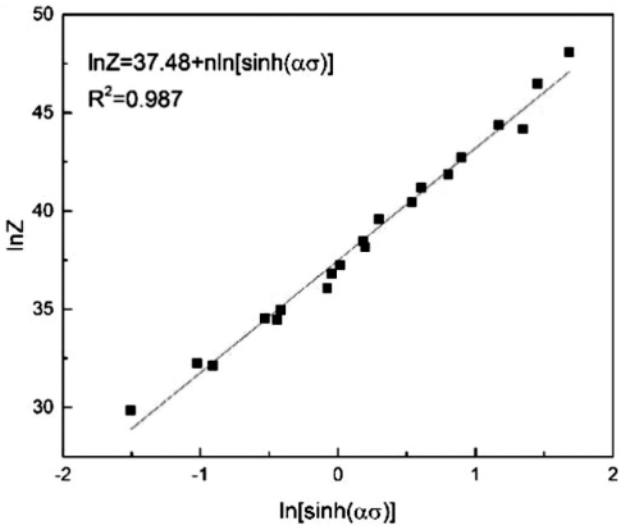

Figure 7: Fitting curve of lnZ–ln[sinh($\alpha\sigma$)]

$$\ln Z = \ln \dot{\varepsilon} + \frac{Q}{RT} = \ln A + n \ln\left[\sinh(\alpha\sigma)\right] \tag{17}$$

Equation (17) is also called the Arrhenius form of the constitutive equation. Hence, the relationship of stable flow stress, deformation temperature, and the strain rate can be expressed as:

$$\sigma = \frac{1}{\alpha} \ln\left\{\left(\frac{Z}{A}\right)^{\frac{1}{n}} + \left[\left(\frac{Z}{A}\right)^{\frac{2}{n}} + 1\right]^{\frac{1}{2}}\right\} \tag{18}$$

When the strain is 0.1, Equation (18) can be written as:

$$\sigma = 51.621 \ln\left\{\left(\frac{\dot{\varepsilon} \exp\left(\frac{221474}{RT}\right)}{1{\cdot}894\times10^{16}}\right)^{0.173} + \sqrt{\left[\left(\frac{\dot{\varepsilon} \exp\left(\frac{221474}{RT}\right)}{1{\cdot}894\times10^{16}}\right)^{0.346} + 1\right]}\right\} \tag{19}$$

As strain has little effect on the flow stress under stable conditions, it does not have to be incorporated into the hyperbolic sine model currently. To make the thermal deformation behavior a more visual and accurate import into the finite-element simulation software, the strain was introduced to the current model.

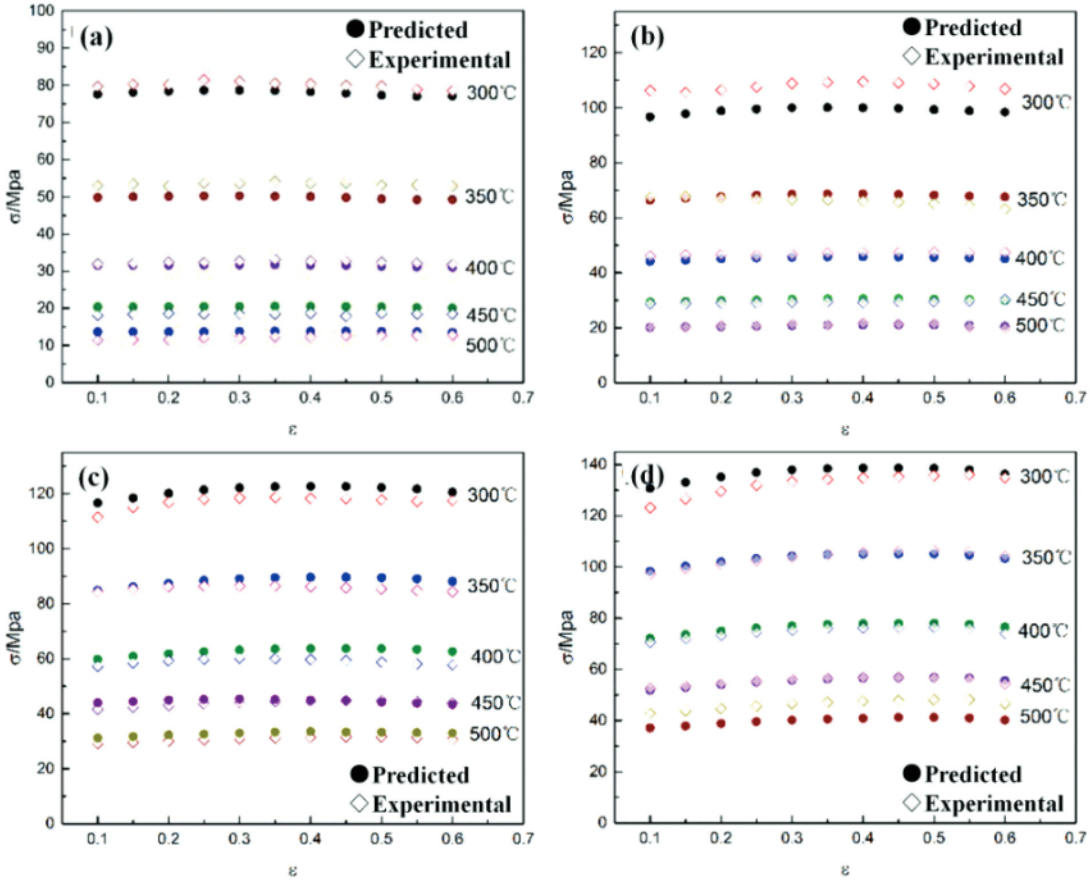

Figure 8: Predicted and experimental value after modification of the true stress under different strain rate: a) 0.01 s^{-1}, b) 0.1 s^{-1}, c) 1 s^{-1}, d) 5 s^{-1}

Polynomial fitting was applied to describe the connection between the parameters and strain in order to calculate the α, n, Q and ln$A$. The results show that quintal polynomial in Equation (20) has good correlation with the parameters above.

$$\begin{cases} \alpha = 0.0184 + 0.0278\varepsilon - 0.253\varepsilon^2 + 0.889\varepsilon^3 - \\ -1.406\varepsilon^4 + 0.8401\varepsilon^5 \\ n = 6.059 - 1.78\varepsilon - 15.873\varepsilon^2 + 90.233\varepsilon^3 - \\ -173.457\varepsilon^4 + 0.8401\varepsilon^5 \\ Q = 222.382 + 115.426\varepsilon - 1859.48\varepsilon^2 + \\ +7385.81\varepsilon^3 - 12767.5\varepsilon^4 + 8211.39\varepsilon^5 \\ \ln A = 38.141 + 9.633\varepsilon - 246.608\varepsilon^2 + \\ +1023.106\varepsilon^3 - 1805.681\varepsilon^4 + 1179.908\varepsilon^5 \end{cases} \quad (20)$$

3.4 The accuracy of constitutive equation

The relationships between the true stress, the temperature, and the strain rate were determined according to the model established when the true strains were 0.1–0.6. Meanwhile, the values are compared to the measured true stress after being modified, as depicted in **Figure 8**. The constitutive equation commonly has a high accuracy in predicting the mechanical performance of the material. To further demonstrate the accuracy of the constitutive equation, the Correlation Coefficient (R) and the Average Relative Error (ARE) are introduced:

$$R = \frac{\sum_{i=1}^{N}(E_i - \overline{E})(C_i - \overline{C})}{\sqrt{\sum_{i=1}^{N}(E_i - \overline{E})^2 \sum_{i=1}^{N}(C_i - \overline{C})}} \quad (21)$$

$$ARE(\%) = \frac{1}{N}\sum_{i=1}^{N}\left|\frac{(C_i - E_i}{E_i}\right| \times 100\% \quad (22)$$

where N represents the number of calculated data; E and $\overline{E}$ are the modified and average values, respectively; C and $\overline{C}$ are the predicted and average values calculated from the constitutive equation.

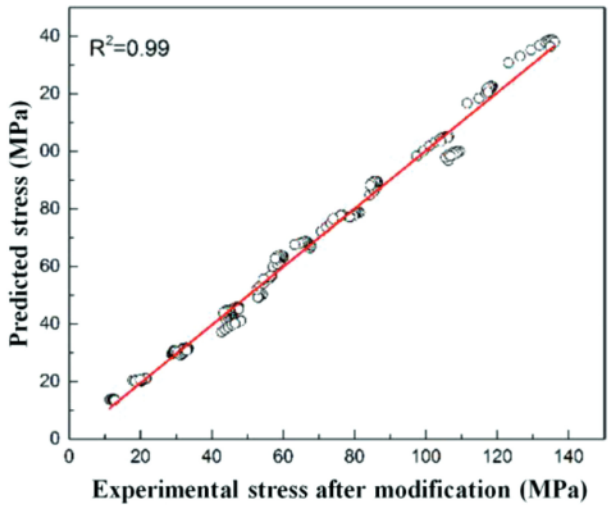

Figure 9: Evaluation of the relevance between the experimental stress after modification and the predicted stress

Figure 9 shows the relevance between the experimental stress after modification and the predicted stress. The Correlation Coefficient (R) equals 0.99, which shows high consistency. The true stress under different strain from 0.1 to 0.6 was calculated and according to Equation (22), the Average Relative Error (ARE) equals 4.8 %.

4 CONCLUSIONS

The thermal-deformation behavior of the A356 aluminum alloy with a Sr modification was investigated, the influences of friction and adiabatic temperature on the true stress-strain curves were modified, and the constitutive equation of the A356 aluminum alloy with Sr modification was proposed. The fitting accuracy of the constitutive equation is high enough to characterize the thermal-deformation behavior of this aluminum alloy. The following conclusions can be drawn:

1) The thermal-deformation of the A356 aluminum alloy with a Sr modification was investigated with a deformation temperature of 300–500 °C and a deformation rate of (0.01, 0.1, 1 and 5) s^{-1}. The flow stress obviously was influenced by both the temperature and the deformation rate.

2) The influences of friction and temperature on the true stress-strain curves were modified. The experimental stresses are lower than that of the theoretical, and the distinction increased with an increase of the strain. The largest gap reaches 17.8 MPa when the sample deformed at 300 °C and 5 s^{-1}, with a decrease of 16 %.

3) The constitutive equation was created after the modification of friction and temperature based on the hyperbolic sine model. The activation energy of the A356 aluminum alloy with a Sr modification Q = 221.474 kJ/mol. The correlation coefficient R is 0.99, and the average relative error (ARE) is 4.8 %, which shows the high relevance of the current model.

Acknowledgement

This work was supported by the Advanced Materials Financial Project of "Technological Innovation 2025" provided by Ningbo Government (2019B10099).

Data availability

The experimental data used to support the findings of this study are included in the article. The other data are available from the corresponding author upon request.

Conflicts of interest

The authors declare that they have no conflicts of interest.

5 REFERENCES

[1] I. Öztürk, G. H. Ağaoğlu, E. Erzi, D. Dispinar, G. Orhan, Effects of strontium addition on the microstructure and corrosion behavior of A356 aluminum alloy, J. Alloy Compd., 763 (**2018**), 384–391, doi:10.1016/j.jallcom.2018.05.341

[2] C. Lee, Effect of strain rate on fatigue property of A356 aluminium casting alloys containing pre-existing micro-voids, Int. J. Fatigue, 131 (**2020**), 105368, doi:10.1016/j.ijfatigue.2019.105368

[3] M. Cardinale, D. Maccio, G. Luciano, E. Canepa, P. Traverso, Thermal and corrosion behavior of as cast AlSi alloys with rare earth elements, J. Alloy Compd., 695 (**2017**), 2180–2189, doi:10.1016/j.jallcom.2016.11.066

[4] B. E. Slattery, T. Perry, A. Edrisy, Microstructural evolution of a eutectic Al-Si engine subjected to severe running conditions, Mater. Sci. Eng. A, 512 (**2009**), 76–81, doi:10.1016/j.msea.2009.01.025

[5] R. Arrabal, B. Mingo, A. Pardo, M. Mohedano, E. Matykina, I. Rodríguez, Pitting corrosion of rheocast A356 aluminium alloy in 3.5 wt.% NaCl solution, Corros. Sci., 73 (**2013**), 342–355, doi:10.1016/j.corsci.2013.04.023

[6] S. Hafenstein, E. Werner, Direct aging of a hot isostatically pressed A356 aluminum cast alloy, Mater. Sci. Eng. A, 768 (**2019**), 138417, doi:10.1016/j.msea.2019.138417

[7] R. Gecu, S. Acar, A. Kisasoz, K. Altug Guler, A. Karaaslan, Influence of T6 heat treatment on A356 and A380 aluminium alloys manufactured by thixoforging combined with low superheat casting, Tran. Nonferr. Metal. Soc., 28 (**2018**), 385–392, doi:10.1016/S1003-6326(18)64672-2

[8] L. Heusler, W. G. Schneider, Influence of alloying elements on the thermal analysis results of Al-Si cast alloys, J. Light Meter., 2 (**2002**), 17–26, doi:10.1016/S1471-5317(02)00009-3

[9] W. R. Osorio, R. L. Garcia, P. R. Goulart, A. Garcia, Effects of eutectic modification and T4 heat treatment on mechanical properties and corrosion resistance of an Al-9 wt.% Si casting alloy, Mater. Chem. Phys., 106 (**2007**), 343–349, doi:10.1016/j.matchemphys.2007.06.011

[10] Z. Shi, Q. Wang, Y. Shi, G. Zhao, R. Zhang, Microstructure and mechanical properties of Gd-modified A356 aluminum alloys, J. Rare Earth, 33 (2015), 1004–1009, doi:10.1016/S1002-0721(14)60518-4

[11] Y. C. Tsai, C. Y. Chou, S. L. Lee, C. K. Lin, J. C. Lin, S. W. Lim, Effect of trace La addition on the microstructures and mechanical properties of A356 (Al-7Si-0.35Mg) aluminum alloys, J. Alloy Compd., 487 (**2009**), 157–162, doi:10.1016/j.jallcom.2009.07.183

[12] S. Shivkumar, L. Wang, D. Apelian, Molten metal processing of advanced cast aluminum alloys, JOM, 43 (**1991**), 26–32, doi:10.1007/BF03220114

[13] R. Ebrahimi, A. Najafizadeh, A new method for evaluation of friction in bulk metal forming, J. Mater. Process. Tech., 152 (**2004**), 136–143, doi:10.1016/j.jmatprotec.2004.03.029

[14] J. Zhang, H. Di, X. Wang, Y. Cao, J. Zhang, T. Ma, Constitutive analysis of the hot deformation behavior of Fe-23Mn-2Al-0.2C twinning induced plasticity steel in consideration of strain, Mater. Design, 44 (**2013**), 354–364, doi:10.1016/j.matdes.2012.08.004

[15] C. Wang, F. Yu, D. Zhao, X. Zhao, L. Zuo, Hot deformation and processing maps of DC cast Al–15%Si alloy, Mater. Sci. Eng. A, 577 (**2013**), 73–80, doi:10.1016/j.msea.2013.04.015

[16] R. L. Goetz, S. L. Semiatin, The adiabatic correction factor for deformation heating during the uniaxial compression test, J. Mater. Eng. Perform., 10 (**2001**), 710–717, doi:10.1361/105994901770344593

[17] C. Devadas, D. Baragar, G. Ruddle, The thermal and metallurgical state of steel strip during hot rolling: Part II. Factors influencing rolling loads, Metall. Mater. Trans. A, 22 (**1991**), 321–333, doi:10.1007/BF02656801

[18] L. Jia, X. Ren, H. Hou, Y. Zhang, Microstructural evolution and superplastic deformation mechanisms of as-rolled 2A97 alloy at low-temperature, Mater. Sci. Eng. A, 759 (**2019**), 19–29, doi:10.1016/j.msea.2019.04.102